JTTEE5 24:659–670
DOI: 10.1007/s11666-015-0216-4
1059-9630/$19.00 © ASM International

Simulation of Motion, Heating, and Breakup of Molten Metal Droplets in the Plasma Jet at Plasma-Arc Spraying

M.Yu. Kharlamov, I.V. Krivtsun, V.N. Korzhyk, Y.V. Ryabovolyk, and O.I. Demyanov

(Submitted April 10, 2014; in revised form November 16, 2014)

The mathematical model for the process of plasma-arc wire spraying is proposed, which describes behavior of molten metal droplets in the plasma jet, allowing for the processes of their deformation and gas-dynamic breakup. Numerical analysis of the processes of motion, heating, and breakup of molten metal droplets, detached from the sprayed wire at plasma-arc spraying of coatings, was performed. It is shown that during molten droplets movement in the plasma jet their multiple breakup takes place, leading to formation of sprayed particles with dimensions much smaller than dimensions of initial droplets, detached from the sprayed wire tip.

Keywords droplet breakup, mathematical modeling, molten droplets, motion and heating of particles, plasma-arc wire spraying

1. Introduction

Industry has recently shown considerable interest in plasma and plasma-arc processes associated with spraying of wires and rods. In particular, the problems of spraying wire and rod consumables are encountered in the processes of coating deposition, as well as producing superfine powders. The fact that already completely molten metal particles penetrate into the flow should be regarded as one of the features of coating spray deposition using wire consumables, unlike the processes of thermal powder spraying, in which powder particles in the solid state are injected into the flow of gas or plasma (Ref 1). Moreover, plasma-arc wire spraying opens up broad capabilities of controlling the characteristics of droplets detached from the tip of sprayed wire or rod by changing the conditions of their feeding into the plasma arc. Alongside that, it should be noted that molten metal particles moving in the high-speed plasma jet are deformed and inner motion develops in them, leading to their destruction with formation of finer fragments (Ref 2). Thermal and dynamic interaction of plasma flow with liquid particles also can differ from its respective interaction with solid particles. All this affects the final result of the spraying process. In particular, the structure and properties of coatings formed in such a spraying process are determined in many respects by the dimensions, velocity, and temperature of liquid particles at their collision with the substrate. On the other hand, in a similar process of dispersion of wire and rods to produce fine and superfine powders, it is necessary to achieve the specified fractional composition of disperse phase. Therefore, study of the processes occurring during movement of molten metal particles in the plasma flow is of great importance for further development of plasma and plasma-arc material processing technologies, associated with spraying of wire materials.

At present, the best studied processes are those of motion and heating of solid spherical particles in the gas and plasma flows. Mathematical models describing acceleration and movement trajectories, as well as heating and melting of such particles in the plasma jet, have been developed (Ref 3–6). Features of thermal interaction of plasma with evaporating and exothermally reacting particles of dispersed material have been investigated (Ref 6). Heating of dispersed particles which are exposed to laser irradiation, as well as combined laser-plasma impact, has been studied (Ref 7). As for behavior of molten particles in the plasma jet, this question has been investigated to a much smaller degree. In particular, one can mention study (Ref 8) which proposes the mathematical model of movement, heating, and oxidation of particles at wire-arc spraying (electric-arc metalizing). At the same time, many features of gas-dynamic and thermal interaction of liquid particles with plasma flow still have not been studied. Therefore, the objective of this study is to develop mathematical models, as well as conducting detailed numerical analysis of the processes of movement, heating, and fragmentation of molten metal droplets in the plasma jet for the conditions of plasma-arc wire spraying.

M.Yu. Kharlamov, I.V. Krivtsun, V.N. Korzhyk, Y.V. Ryabovolyk, and **O.I. Demyanov**, E.O.Paton Electric Welding Institute of the NAS of Ukraine, Kyiv, Ukraine. Contact e-mail: mykharlamov@gmail.com.

2. Models of Liquid Particle Movement and Heating in the Plasma Jet

Let us consider the main equations, describing the behavior of molten metal droplets, detached from the sprayed wire tip by the plasma flow. We will assume that the initial parameters of droplets entering the plasma jet are determined proceeding from the conditions of dynamic and thermal interaction of the arc plasma flow with the wire material. In particular, we will assume that the coordinates of the point of liquid particle entering the plasma flow x_0, z_0 (Fig. 1) coincide with the position of molten wire tip, which can be determined from the model presented in (Ref 9). The same model is used to determine initial droplet temperature T_0, which is taken to be equal to the temperature of the melt contained at sprayed wire tip. In its turn, initial values of diameter d_0 and velocity $\mathbf{w}_0$ of movement of a liquid particle formed at wire dispersion are determined on the basis of a model of jet flow of molten wire metal and formation of molten metal droplets in the concurrent high-velocity gas flow (Ref 10).

We will use the approximation of the low-dusted jet to describe the influence of plasma jet on a droplet of molten metal at its motion, heating, and breakup in the plasma jet (Ref 7, 11), i.e., the effect of the loss of momentum and energy of the jet due to its interaction with the entire set of particles (droplets) will be neglected. In addition, it is assumed that collisions of the particle and its fragments with other particles (fragments) are improbable.

After detachment of droplets, their movement in the plasma jet is described by the following equations (Ref 3):

$$\frac{d(m\mathbf{w})}{dt} = \mathbf{F}; \quad \frac{d\mathbf{r}}{dt} = \mathbf{w}. \qquad \text{(Eq 1)}$$

Here, $m(t)$, $\mathbf{w}(t) = (w_x, w_y, w_z)$, and $\mathbf{r}(t) = (x, y, z)$ are the current values of mass ($m(0) \equiv m_0 = \frac{4}{3}\pi d_0^3 \rho_m$, where ρ_m is the molten metal density), velocity vector, and radius-vector of particle position in the selected Cartesian system of coordinates (see Fig. 1); $\mathbf{F}(t)$ is the resulting force acting on the liquid particle from the plasma side.

It was assumed that the main force acting on the particle is the aerodynamic drag force (Ref 12):

$$\mathbf{F} = 0.5\, C_d S \rho (\mathbf{v} - \mathbf{w})|\mathbf{v} - \mathbf{w}|, \qquad \text{(Eq 2)}$$

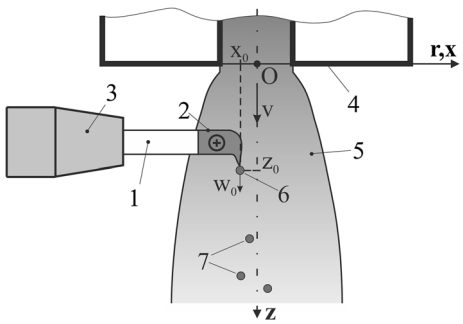

Fig. 1 Schematic of particle entering into the plasma flow in plasma-arc wire spraying: 1—sprayed wire, 2—molten part of the wire, 3—holder, 4—plasmatron nozzle, 5—plasma jet, 6—droplet detaching from molten wire tip, 7—droplets-particles in the plasma flow

where C_d is the aerodynamic drag coefficient; S is the cross-sectional area of the particle; $\mathbf{v}$ is the vector of undisturbed plasma velocity in the particle location point, ρ is the plasma density.

One of the features of liquid particles motion in the gas (plasma) flow is the fact that as a result of flow influence the particle is deformed, thus changing its midsection, as well as coefficient C_d. This leads to a change of the aerodynamic drag force $\mathbf{F}$ acting on the particle (Ref 2, 13, 14). Let us assume that when moving in the plasma jet, the liquid particle, while deforming, takes the shape of an ellipsoid of revolution (oblate spheroid) (Fig. 2), the geometrical dimensions of which will be characterized by dimensionless parameter

$$y = \frac{d_{mid}}{d_V}, \qquad \text{(Eq 3)}$$

which is the ratio of particle midsection diameter d_{mid} to diameter of a sphere of equivalent volume d_V. Thus, particle midsection area will be given by

$$S = \pi d_V^2 y^2 / 4. \qquad \text{(Eq 4)}$$

To take into account the changes of liquid particle shape at its movement in the plasma flow, we will use the equation proposed in the study (Ref 13):

$$\frac{\pi^2 + \frac{16}{y^6}}{\pi^2 + 16}\frac{d^2 y}{d\tilde{t}^2} - \frac{48}{\pi^2 + 16}\frac{1}{y^7}\left(\frac{dy}{d\tilde{t}}\right)^2 + \frac{40}{\mathrm{Re}_{def}}\frac{1}{y^2}\frac{dy}{d\tilde{t}} + \frac{20}{\mathrm{We}}\frac{1}{S_0}\frac{dS}{dy} = \frac{2C_2}{y}. \qquad \text{(Eq 5)}$$

Here, $\tilde{t} = t/t^*$ is the dimensionless time; $t^* = \frac{d_V}{|\mathbf{v}-\mathbf{w}|}\sqrt{\frac{\rho_m}{\rho}}$ is the characteristic breakup time (Ref 2); $C_2 = 2/3$; $\mathrm{Re}_{def} = |\mathbf{v} - \mathbf{w}| \cdot d_V / \eta_m \cdot \sqrt{\rho \cdot \rho_m}$ is the Reynolds number for melt flow in the droplet (Ref 13); η_m is the dynamic viscosity of molten particle material; We is the Weber number, defined as

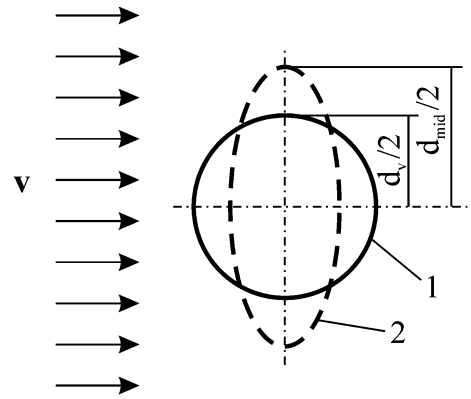

Fig. 2 Schematic representation of molten particle shape at particle movement in the plasma jet: 1—sphere (undeformed state); 2—oblate spheroid (deformed state)

$$\mathrm{We} = \frac{|\mathbf{v} - \mathbf{w}|^2 d_V \rho}{\sigma}, \qquad \text{(Eq 6)}$$

where σ is the coefficient of surface tension of the droplet liquid metal. Initial conditions required for solution of Eq 5 are assigned as follows:

$$y(0) = 1, \ \left.\frac{dy}{d\tilde{t}}\right|_{\tilde{t}=0} = 0. \qquad \text{(Eq 7)}$$

Let us describe the method of calculation of aerodynamic drag coefficient C_d for the liquid particle, which would allow for the features of plasma and plasma-arc processes of wire spraying. In particular, it is necessary to take into account droplet deformation, as well as a broad range of variation of the Reynolds number Re, determined as

$$\mathrm{Re} = (\rho\,|\mathbf{v} - \mathbf{w}|\,d_V)/\eta, \qquad \text{(Eq 8)}$$

where η is the dynamic viscosity of plasma in the point of particle location. For this purpose, we will use interpolation polynomial proposed in (Ref 15). This polynomial allows the calculation of C_d for an ellipsoid by the known aerodynamic drag coefficients for disk $C_{d_{Disk}}$, sphere $C_{d_{Sphere}}$ and flattened spheroid with form factor $E = 0.5$, $C_{d_{0.5}}$:

$$C_d = 2(E-1)(E-0.5)\cdot C_{d_{Disk}} - 4E(E-1)C_{d_{0.5}} + 2E(E-0.5)\cdot C_{d_{Sphere}}, \qquad \text{(Eq 9)}$$

where $E = 1/y^3$ is the aspect ratio of the particle shape ($E = 1$ for a sphere, $E \simeq 0$ for a disk). As a result, expression (9) takes into account the droplet shape change at its movement in the plasma flow, using known dependencies for determination of $C_{d_{Disk}}$, $C_{d_{Sphere}}$, and $C_{d_{0.5}}$ values. In particular, to determine the aerodynamic drag coefficient of a spherical particle $C_{d_{Sphere}}$, we will use dependencies (Ref 14), allowing calculations to be performed for a large range of variation of the number Re:

$$C_{d_{Sphere}} = \begin{cases} \frac{24}{\mathrm{Re}}, & \mathrm{Re} < 0.01, \\ \frac{24}{\mathrm{Re}}\left(1 + 0.1315\mathrm{Re}^{0.82-0.05\lg \mathrm{Re}}\right), & 0.01 < \mathrm{Re} \le 20, \\ \frac{24}{\mathrm{Re}}\left(1 + 0.1935\mathrm{Re}^{0.6305}\right), & 20 < \mathrm{Re} \le 260, \\ 10^{1.6425 - 1.1242\lg \mathrm{Re} + 0.1558\lg^2 \mathrm{Re}}, & 260 < \mathrm{Re} \le 1500, \\ 10^{-2.4751 + 2.5558\lg \mathrm{Re} - 0.9295\lg^2 \mathrm{Re} + 0.1049\lg^3 \mathrm{Re}}, & 1500 < \mathrm{Re} \le 1.2 \times 10^4. \end{cases} \qquad \text{(Eq 10)}$$

We will determine aerodynamic drag coefficient of a disk $C_{d_{Disk}}$ from expression (Ref 16)

$$C_{d_{Disk}} = \begin{cases} \frac{64}{\pi \mathrm{Re}}\left(1 + 0.138\mathrm{Re}^{0.792}\right), & 1.5 \le \mathrm{Re} \le 100, \\ \frac{64}{\pi \mathrm{Re}}\left(1 + 0.00871\mathrm{Re}^{1.393}\right), & 100 \le \mathrm{Re} \le 300, \\ 1.17, & \mathrm{Re} > 300, \end{cases} \qquad \text{(Eq 11)}$$

and for drag coefficient of a flattened ellipsoid $C_{d_{0.5}}$ we will use the following formula (Ref 16)

$$\log_{10} C_{d_{0.5}} = 2.0351 - 1.660\log_{10} \mathrm{Re} + 0.398(\log_{10} \mathrm{Re})^2 - 0.0306(\log_{10} \mathrm{Re})^3. \qquad \text{(Eq 12)}$$

The thermal state of particles at plasma-arc spraying is determined from the non-stationary heat conduction equation, allowing for the influence of convective, conductive and radiation heat exchange of plasma flow with particle surface, as well as heat losses associated with removal of the energy of particle material atom evaporation by vapor flow. In the first approximation, for temperature field calculation we will assume a spherical shape of a particle, using current value of diameter of a sphere of equivalent volume d_V. Use of this approximation is caused by a task to receive, first of all, an average temperature field in a particle that would allow tracking changes in its thermal state at particle movement along the spraying distance, taking into account the possible fragmentation, as well as assessment of the mean bulk temperature of the material forming the coating.

Considering the made assumptions, the non-stationary heat conduction equation for determination of space–time distribution of temperature in such a particle will look like

$$\rho_m \bar{C}_m \frac{\partial T_m}{\partial t} = \frac{1}{r^2}\frac{\partial}{\partial r}\left(r^2 \chi_m \frac{\partial T_m}{\partial r}\right). \quad \text{(Eq 13)}$$

Here, $T_m(r, t)$ is the space-time distribution of temperature in the particle; $\chi_m(T)$ and $\bar{C}_m(T)$ are the coefficient of heat conductivity and effective heat capacity of particle material, determined as

$$\bar{C}_m = c_m(T) + W^{(m)}\delta\left(T - T^{(m)}\right), \quad \text{(Eq 14)}$$

where $c_m(T)$ is the specific heat capacity of material; $T^{(m)}$ is the melting temperature; $W^{(m)}$ is the latent heat of melting; $\delta(x)$ is the delta function. The essence of the effective heat capacity determined by formula (14) is set forth in the study (Ref 17): substitution of (14) into the heat conduction Eq 13 transforms the latter into enthalpy form, allowing application of the shock-capturing method, without the need for obvious allocation of interface boundaries.

Boundary conditions for Eq 13 have the following form:

$$-\left(\chi_m \frac{\partial T_m}{\partial r}\right)\Big|_{r=a} = Q_c + Q_r - Q_v, \qquad \frac{\partial T_m}{\partial r}\Big|_{r=0} = 0, \quad \text{(Eq 15)}$$

where $a(t) = d_V(t)/2$ is the current radius which can vary as a result of particle material evaporation; $Q_c(t)$, $Q_r(t)$, and $Q_v(t)$ are the convective-conductive, and radiation heat flows, as well as specific heat losses associated with surface evaporation of particle material.

Initial condition, required for solution of Eq 13, is assigned as

$$T_m(r)|_{t=0} = T_0 \geq T^{(m)}, \quad \text{(Eq 16)}$$

where T_0 is the initial particle temperature, taken to be equal to the temperature of the melt, detached from the sprayed wire tip, which can be determined by model (Ref 9).

Let us determine the components of heat exchange between plasma and particles. So, the density of energy flow due to convective-conductive heat exchange of particle surface with the plasma can be determined on the basis of Newtonian model of heat transfer (Ref 18):

$$Q_c = \alpha(T_p - T_{ms}), \quad \text{(Eq 17)}$$

where T_p is the temperature of undisturbed plasma flow, T_{ms} is the temperature of particle surface, α is the heat exchange coefficient related to Nusselt number by the following relationship (Ref 2, 3):

$$\mathrm{Nu} = (\alpha d_V)/\chi, \quad \text{(Eq 18)}$$

where χ is the coefficient of heat conductivity of plasma calculated at the temperature of undisturbed flow. Nu number can be calculated based on the following dependence (Ref 19):

$$\mathrm{Nu} = 2\frac{\chi_s}{\chi} + 0.5\mathrm{Re}^{0.5}\mathrm{Pr}^{0.4}\left(\frac{\rho\eta}{\rho_s\eta_s}\right)^{0.2}. \quad \text{(Eq 19)}$$

Here, $\mathrm{Pr} = (C_p\eta)/\chi$ is the Prandtl number; C_p is the heat capacity of plasma in the point of particle location; index s denotes plasma properties determined at particle surface temperature.

The resulting thermal radiation energy flux is calculated from the following expression (Ref 18):

$$Q_r = \beta\sigma_0\left(T_p^4 - T_{ms}^4\right), \quad \text{(Eq 20)}$$

where β is the degree of blackness of wire material; σ_0 is the Stefan-Boltzmann constant.

Heat flux due to material evaporation from molten particle surface can be calculated by the following expression:

$$Q_v = \varepsilon n u, \quad \text{(Eq 21)}$$

where ε is the latent heat of evaporation per one atom; n, u are the concentration and velocity of metal vapor atoms near the evaporating surface, determined by the procedure described in (Ref 20).

3. Breakup of Molten Particles in the Plasma Jet

Let us consider the conditions, at which molten particle breakup takes place in the plasma flow. Weber number We is the most important of the characteristic parameters, determining the stability and destruction of droplets (Ref 2, 21). Depending on We values, several breakup modes (or mechanisms) are determined, limited by critical values of We* number (Ref 2, 22):

(1) vibrational breakup We = 8-12;
(2) bag breakup $12 < \mathrm{We} < 50$;
(3) bag-and-stamen breakup $50 < \mathrm{We} < 100$;
(4) sheet stripping $100 < \mathrm{We} < 350$;
(5) wave crest stripping $\mathrm{We} > 350$;
(6) catastrophic breakup $\mathrm{We} > 350$.

Performed quantitative estimates show that in plasma-arc wire spraying Weber number for a molten particle moving in the plasma flow can vary in the range of 0-80 (Ref 23). That is, under the conditions of plasma-arc spraying, the most characteristic modes of liquid particle breakup are vibrational breakup, as well as bag and bag-and-stamen breakup.

Note that the above ranges of We number values are quite conditional and in literature the critical We* values (at which a particular breakup mechanism is manifested) show considerable scatter (Ref 21). Nonetheless, in study (Ref 21) a generalized dependence is proposed for We* determination, which exactly was used to construct the model of molten particle breakup in the plasma jet. A

similarity criterion, based on averaged in time Weber number, is introduced (Ref. 11) for quantitatively allowing of the interaction of the flow on droplet-particle

$$H = t_{\mathrm{k}}^{-1} \int_0^{t_{\mathrm{cr}}} \mathrm{We}(t)dt, \qquad \text{(Eq 22)}$$

where the integral is taken from the start of the action of aerodynamic forces on the droplet up to moment t_{cr} of achievement of critical values of Weber number We*. Here, t_{k} is the period of natural vibrations of the droplet, which according to (Ref 2) can be defined as

$$t_{\mathrm{k}} = 0.25\pi \left\{ \frac{\sigma}{\rho_{\mathrm{m}} d_{\mathrm{V}}^3} - 6.25 \frac{\eta_{\mathrm{m}}^2}{\left(\rho_{\mathrm{m}} d_{\mathrm{V}}^2\right)^2} \right\}^{-0.5}. \qquad \text{(Eq 23)}$$

In its turn, We* value, at which droplet breakup takes place, was determined using equation (Ref 21)

$$\mathrm{We}^* = \begin{cases} 13.54 - 0.442L, & \text{if } H \le H' \\ (17.04 - 0.556L)\exp(-(0.028 + 0.00486L)H), & \\ \text{if } H' \le H \le 12.7 & \end{cases}$$
$$L = \ln \mathrm{La}, \quad H' = 6.41 - 0.331L, \qquad \text{(Eq 24)}$$

where $\mathrm{La} = d_{\mathrm{V}} \rho_{\mathrm{m}} \sigma / \eta_{\mathrm{m}}$ is the Laplace number.

Droplet breakup occurs not instantly, but has a certain time interval, which starts from moment t_{cr} of the droplet reaching critical values of We number and ends after complete breakup of the droplet. Studies (Ref 2, 21, 22) give some results of measurement of the time of droplet total destruction t_{b} (breakup time), dependent in the general case on determinant breakup criteria (We, La numbers, etc.), as well as breakup mode. In this study, we will determine t_{b} value using the results of (Ref 22)

$$\tilde{t}_{\mathrm{b}} = t_{\mathrm{b}}/t^* = \begin{cases} 6(\mathrm{We} - 12)^{-0.25}, & 12 \le \mathrm{We} \le 18, \\ 2.45(\mathrm{We} - 12)^{0.25}, & 18 \le \mathrm{We} \le 45, \\ 14.1(\mathrm{We} - 12)^{0.25}, & 45 \le \mathrm{We} \le 351, \\ 0.766(\mathrm{We} - 12)^{0.25}, & 351 \le \mathrm{We} \le 2670, \\ 5.5, & \mathrm{We} \ge 2670. \end{cases} \qquad \text{(Eq 25)}$$

In addition, important time characteristics of the process of droplet breakup include time of breakup induction t_{i} (breakup delay), after which breakup becomes noticeable (Ref 2) and which is calculated from moment t_{cr}. Time t_{i} was used in calculations to determine the upper time limit of the applicability of Eq 5, allowing for the change of shape of a molten particle, which began to break up. Value t_{i} was found from the following equation (Ref 24)

$$\tilde{t}_{\mathrm{i}} = t_{\mathrm{i}}/t^* = 1.5. \qquad \text{(Eq 26)}$$

It was believed that the particle is breaking up after time t_{b} has elapsed since the moment of molten particle achieving critical values of Weber number. Here, it was assumed that the velocity of forming fragments is equal to that of the particle before its breakup, and fragments have a spherical shape. Initial temperature $(T_{\mathrm{i}})_0$ of fragments was taken to be equal to volume-averaged temperature of initial particle at the moment of particle breakup, defined as

$$T = \frac{3}{a^3} \int_0^a T(r) r^2 dr. \qquad \text{(Eq 27)}$$

This is attributable to mixing of droplet liquid metal during its breakup. In addition, a mandatory condition for particle fragment formation is the mass balance:

$$m_0 = \sum_{i=1}^{n_{\mathrm{f}}} m_i, \qquad \text{(Eq 28)}$$

where m_i is the mass of i-th fragment; n_{f} is the number of formed fragments.

Considerable attention should be given to questions related to the number of forming fragments, as well as their size distributions that are now absolutely insufficiently studied. Binary breakup model is often used in modeling flows with droplet breakup, i.e., it is assumed that at occurrence of critical conditions the initial droplet is divided into two, the volume (mass) of which is determined by the specified law of distribution (Ref 25, 26). At the same time, liquid droplet breaking up by the gas flow usually leads to the formation of a multitude of fragments (Ref 2, 27), the number of which is determined by breakup mode, as well as other factors. Therefore, application of higher order breakage scenarios for description of droplet behavior in the plasma flow would be more correct. An approximate estimate of the number of fragments formed at droplet breakup can be made, using expression (Ref 28) applicable for a wide range of multiphase flows

$$n_{\mathrm{f}} = 2 + 0.9 \left\lfloor \left(\frac{d_{\mathrm{V}}}{d_{\mathrm{cr}}} \right) - 1 \right\rfloor, \qquad \text{(Eq 29)}$$

where d_{cr} is the stable maximum droplet diameter, at which its breakup will not proceed and which can be assessed as follows (Ref 22):

$$d_{\mathrm{cr}} = \mathrm{We}^* \frac{\sigma}{\rho \cdot |\mathbf{v} - \mathbf{w}|^2}. \qquad \text{(Eq 30)}$$

To determine sizes of fragments formed at droplet breakup, we will use the breakage distribution function offered in one of the few studies devoted to the multiple breakups of particles (Ref 29):

$$h(\varphi_1, \varphi_2, \ldots, \varphi_{n_{\mathrm{f}}-1}, k) = \frac{A_p \varphi_1^p \varphi_2^p, \ldots, \varphi_{n_{\mathrm{f}}-1}^p \left(k - \sum_{i=1}^{n_{\mathrm{f}}-1} \varphi_i\right)^p}{k^{n_{\mathrm{f}} \cdot p + n_{\mathrm{f}} - 1}}, \qquad \text{(Eq 31)}$$

where k, ϕ_i are the volumes of initial droplets and fragments, respectively; p is the constant, which was taken to be equal to 1 in calculations (Ref 29).

4. Modeling Results

The described model was used at numerical analysis of behavior of molten metal particles in the plasma jet,

Table 1 Initial parameters of droplets—molten particles detached from the sprayed wire tip

No	I, A	G(Ar), m^3/h	D_w, mm	v_w, m/min	$\bar{d}_0$, μm	$\bar{w}_{x0}$, m/s	$\bar{T}_0$, K	z_0, mm	x_0, mm
1	200	1.0	1.4	7	755	0.75	1774.39	6.3	0.74
2				9	670	1.31	1773.39		0.62
3				12	650	1.85	1774.10		0.48

formed by the plasmatron with the external anode wire. Thermal and gas-dynamic characteristics of plasma jet, required for calculations, were precalculated using an earlier developed mathematical model (Ref 30), at the following operating modes of the plasmatron: arc current $I = 200$ A; plasma gas flow rate (Ar) $G_1 = 1$ m^3/h; blowing gas (air) flow rate $G_2 = 20$ m^3/h. Initial parameters of molten particles detached from the wire tip, including their average diameter $\bar{d}_0$, velocity $\bar{w}_{x0}$, and temperature $\bar{T}_0$, as well as the point of their entering into the plasma flow (x_0, z_0), were determined on the basis of models (Ref 9, 10). During calculations, it was assumed that solid wire from low-carbon steel is sprayed. Wire properties were taken from (Ref 31), its diameter being equal to 1.4 mm, rate of its feeding into the arc was 7-12 m/min, and distance from the wire to plasmatron nozzle edge was 6.3 mm. Data on initial parameters of particles detached from molten wire tip into the plasma flow are summarized in Table 1. Taking into account the specified parameters of modeling of plasma-arc spraying process, we can estimate the applicability of the low-dusted jet approximation, used in the model. This approximation is well justifiable, if the volume fraction of dispersed phase κ does not exceed 4×10^{-4} (Ref 7, 11). In plasma-arc spraying, the estimated wire volumetric rate is $(6\text{-}12) \times 10^{-4}$ m^3/h and total gas flow rate is about 21 m^3/h. In these conditions, the volume fraction of a disperse phase is $(3\text{-}6) \times 10^{-5}$ and justifies the use of the low-dusted jet approximation.

Results of computer modeling of molten metal droplet behavior under the considered conditions are presented in Fig. 3 to 6. Figure 3 gives the calculated values of velocity and temperature of the droplet formed at spraying of 1.4-mm diameter wire at the feed rate of 9 m/min, as well as of fragments formed at droplet breakup at their movement along spraying distance in the region of $6.3 \le z \le 35$ mm. As is seen, molten metal droplet, entering into the high-velocity high-temperature plasma flow, is exposed to critical conditions leading to its fast destruction. During breaking up the destroyed droplet has enough time to move for about 7 mm in the plasma flow and after that, for the case shown in Fig. 3, it breaks up into 6 fragments of 248, 306, 356, 396, 400, and 440 μm diameter. Reduction of fragment mass, compared to that of the initial droplet, intensifies acceleration and heating of formed fragments in the plasma jet. Finer fragments (of 248, 306, 356 μm diameter) also break up shortly, while larger ones (396, 400 and 440 μm) have enough time to cover a longer distance in the plasma jet before their destruction. Further on, multiple secondary breakups of fragments are observed (see Fig. 3). The finest fragments are heated fast enough over their volume up to material boiling temperature, which results in part of formed fragments starting to loose their mass at distance $z > 30$ mm, due to material evaporation from the surface.

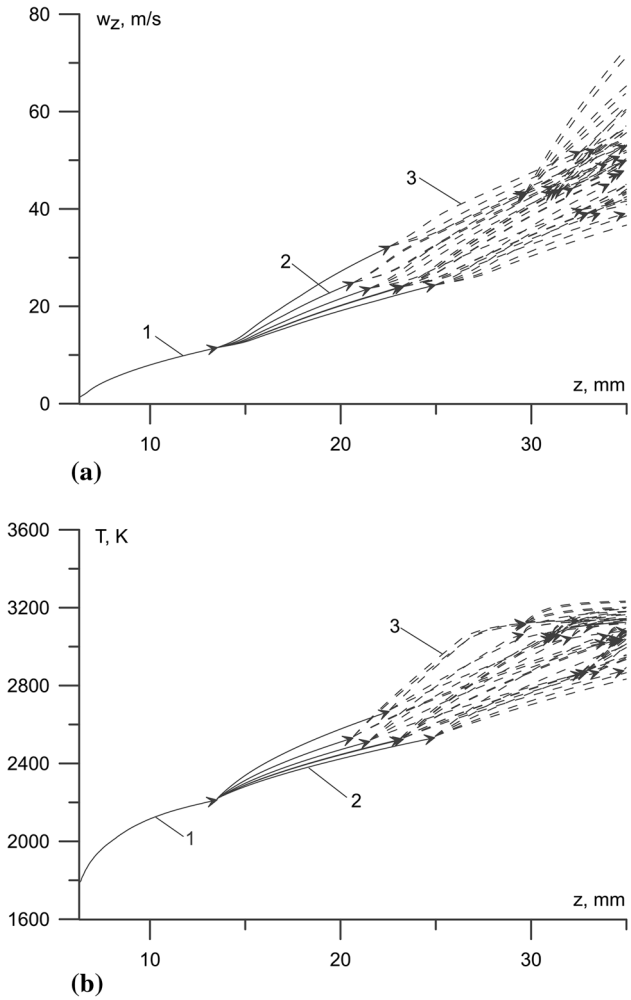

Fig. 3 Change of movement speed (a) and average temperature (b) of initial molten particle, as well as its fragments formed as a result of breakup at movement along spraying distance: 1—initial droplet ($w_0 = 1.31$ m/s, $d_0 = 670$ μm); 2—initial droplet fragments, 3—secondary fragments formed at subsequent breakups

Generalized data on acceleration, heating, and breakup of molten particles and their fragments in the plasma flow are given in Fig. 4. In particular, this Figure shows calculated values of the number of particles in each section of the jet, as well as change of averaged values of velocity, temperature, average diameter, and Weber number along the spraying distance for particles in polydisperse flow, formed at breaking up of a droplet detached from the

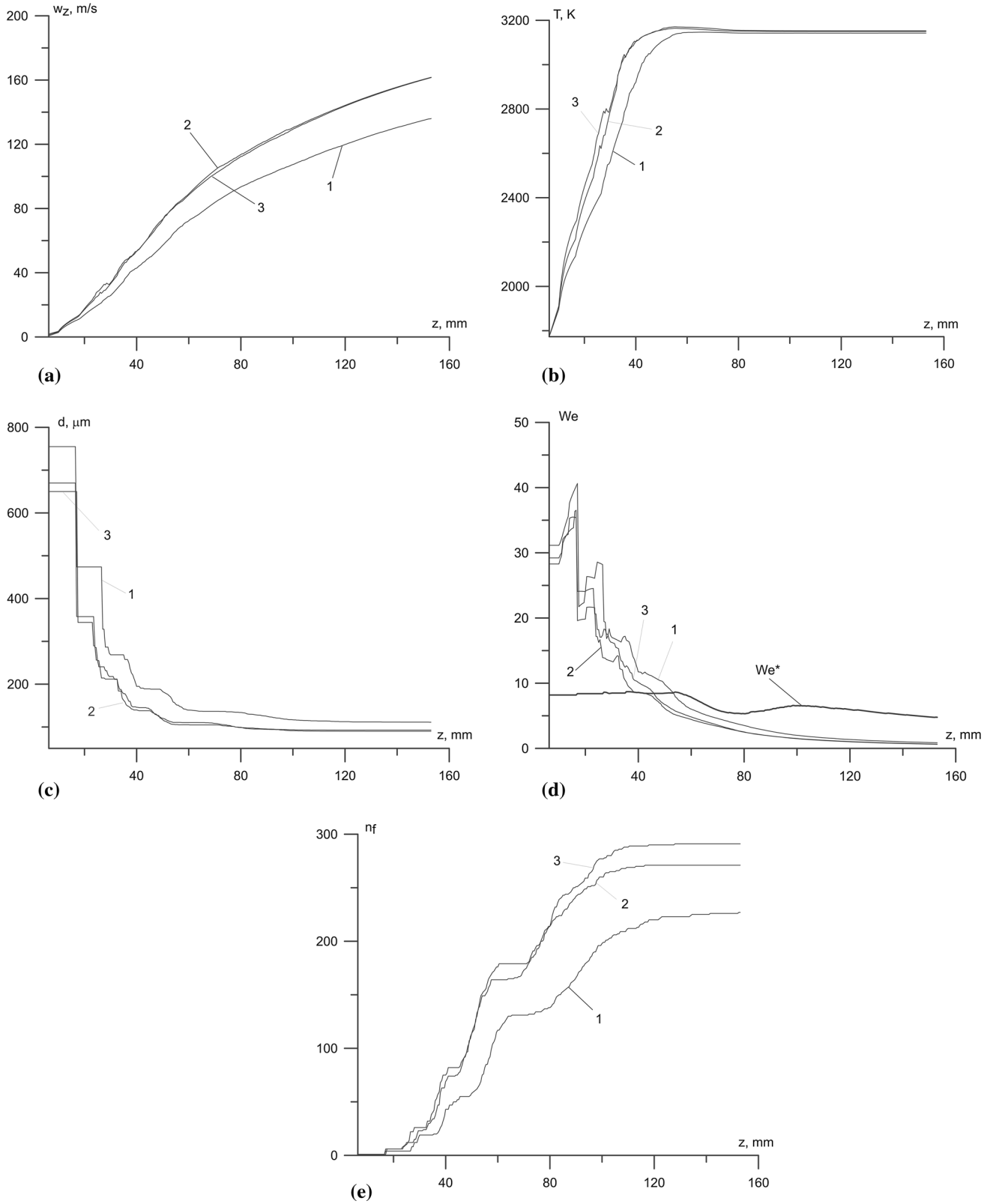

Fig. 4 Change of average values of velocity (a), volume-averaged temperature (b), diameter (c), Weber number (d), as well as number of particles (e) in the dispersed flow, formed at breakup of a droplet detached from the sprayed wire tip along spraying distance: 1—$d_0 = 755$ μm, $w_0 = 0.75$ m/s; 2—$d_0 = 670$ μm, $w_0 = 1.31$ m/s; 3—$d_0 = 650$ μm, $w_0 = 1.85$ m/s

sprayed wire tip under the plasma-arc spraying conditions. The results are given for three modes, differing by wire feed rate v_w and, therefore, also by initial parameters of the droplets detached from the sprayed wire tip (see Table 1). As is seen from the given calculation results, multiple breakups of particles and their fragments moving in the plasma jet take place at plasma-arc spraying. In particular, about 200-300 fragments of average diameter of 90-110 μm are formed from the initial droplets of 670-755 μm diameter over spraying distance of 150 mm, as a result of multiple breakups.

Proceeding from calculation results two most characteristic regions of breakup of liquid particles and their fragments can be singled out. In the first region (near plasmatron nozzle edge), which is characterized by high values of plasma velocity and temperature and at the considered spraying mode has the length of about 60 mm, the most intensive particle breakup takes place (see Fig. 4c, d). In this region, We number for particles is significantly higher than the critical value of Weber number We*, leading to their intensive breakup. In the second region (at z>60mm, see Fig. 4), changes in the particle flow are caused by the reduction (as a result of fragmentation) of particles sizes and by the reduction of the relative velocity of the plasma and particles at increased distance from the nozzle of the plasma torch. Molten particles undergo gradual increase of the aerodynamic drag force due to the change of particle shape that after a certain time can also lead to their destruction. Particles breakup practically always stops at a distance of about 120 mm from the plasmatron nozzle edge; as under corresponding flowing conditions, the time of development of particle deformation and breakup processes becomes commensurable or exceeds the time required for the particles to reach the sprayed surface.

Breakup processes have an essential influence on thermal and dynamic characteristics of sprayed particles. As a result of intensive breakup, practically all the particles in the flow reach boiling temperature already at the distance of ~80 mm from plasmatron nozzle edge (see Fig. 4b). The magnitude of particles acceleration decreases even despite the reduction of the mass of particles as a result of their breakup, which is associated with lowering of plasma jet velocity (Ref 30).

Trajectories of molten particles movement in the plasma jet are of great interest in terms of prediction of spraying material distribution over the spraying spot. As multiple breakups of the initial droplet detached from the molten wire tip result in formation of a cluster consisting of several hundreds of particles of different size, it is extremely difficult to analyze the individual trajectories of their movement. Instead, Fig. 5 shows regions in a plane passing through the wire and the plasma jet axis, in which movement of fragments of initial droplet (fragments spread area) takes place. As is seen from the presented results, the width of fragment movement area gradually increases, when fragments approach the substrate. Transverse dimensions of the region, in which their movement takes place, depend on initial particle size, as well as the point of its entering the plasma flow that is determined by

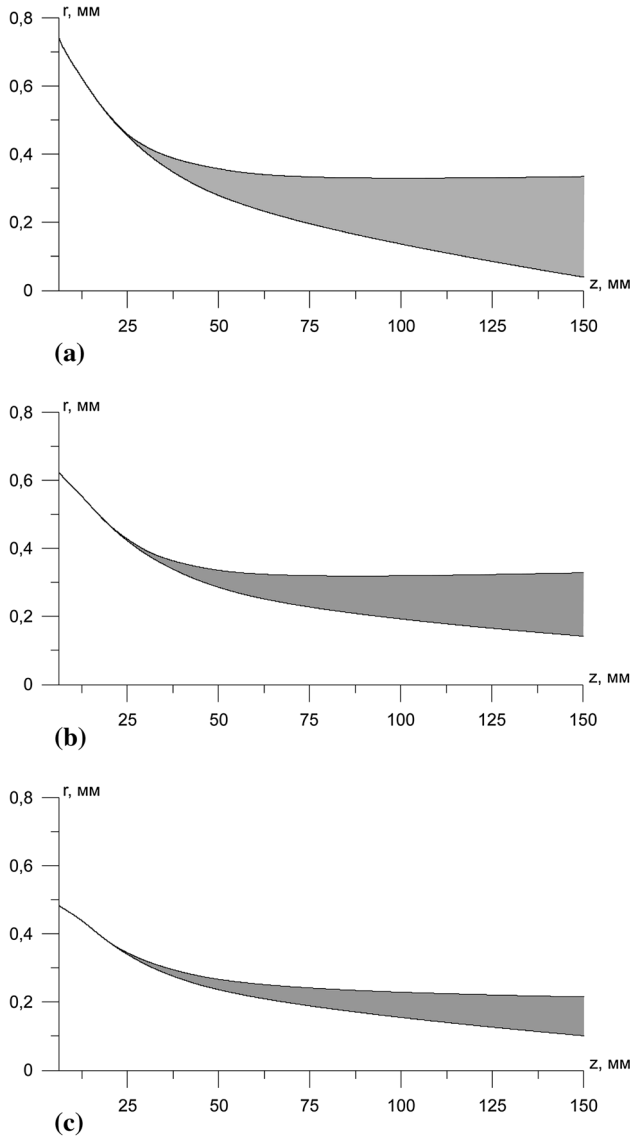

Fig. 5 Regions of motion of the fragments of molten droplet detached from the wire tip (r: distance from the axis of symmetry, z: distance from the edge of the plasma torch): (a)—$d_0 = 755$ μm, $w_0 = 0.75$ m/s; (b)—$d_0 = 670$ μm, $w_0 = 1.31$ m/s; (c)—$d_0 = 650$ μm, $w_0 = 1.85$ m/s

spraying mode parameters. In particular, at breaking off of a large-diameter particle from the molten wire tip that corresponds to low wire feed rates, the fragment spread area becomes wider, along with considerable displacement of particle entrance region relative to the plasma jet axis (see Fig. 5).

Finally, let us consider the distributions of particles, formed as a result of breakup at distance $z = 150$ mm from plasmatron edge (assumed spraying distance), by velocities, temperatures, and dimensions (Fig. 6). Distribution data can be useful at analysis of the conditions of coating deposition, formation of their structure and properties. As follows from this Figure, in spraying mode #1 (see Table 1), when wire feed rate is equal to 7 m/min, the main bulk of particles approaching the substrate has the

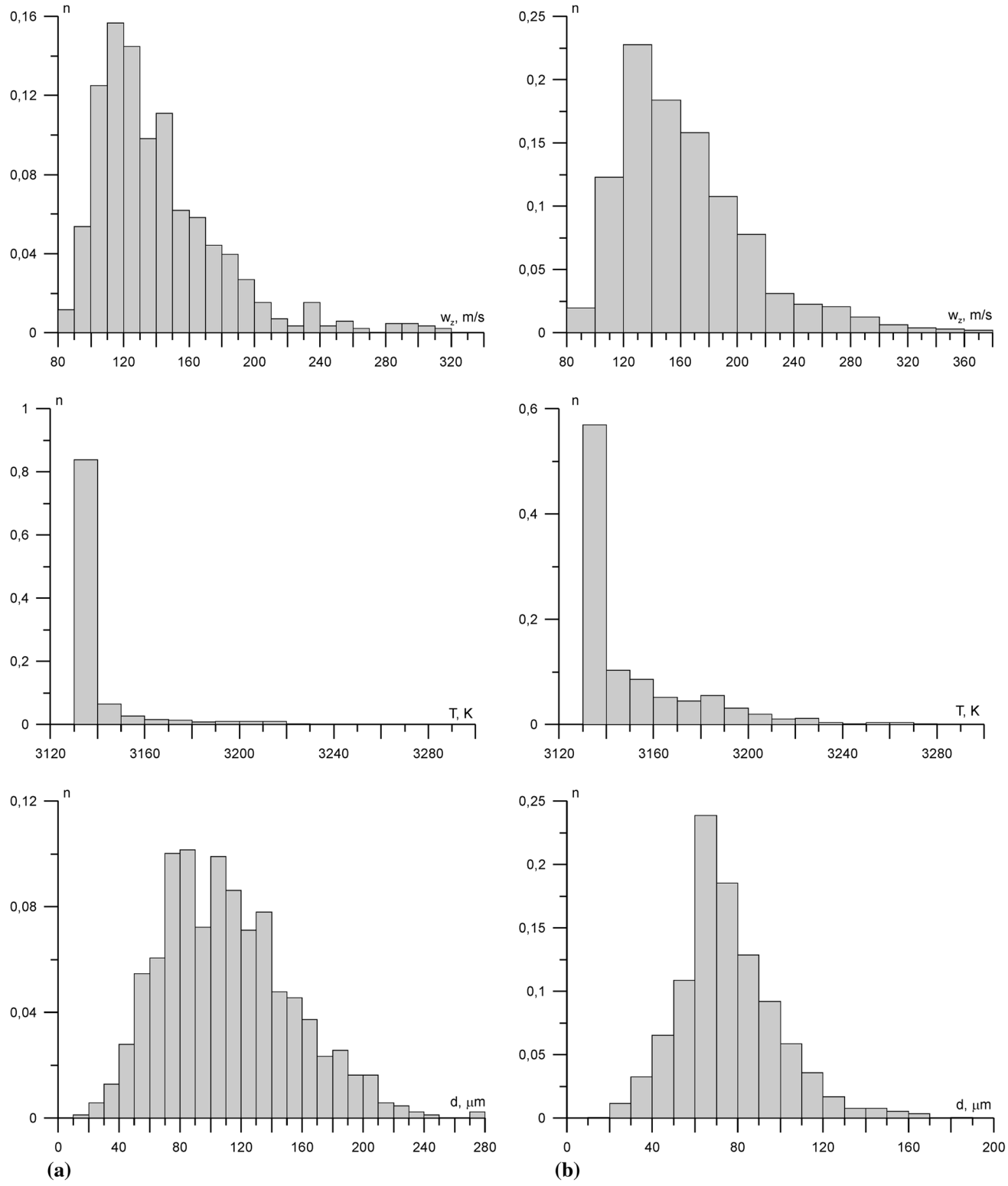

Fig. 6 Distribution of particles formed at breakup of a droplet detached from the sprayed wire tip, by velocities, volume-averaged temperatures and diameters at spraying distance of 150 mm: (a)—$d_0 = 755$ μm, $w_0 = 0.75$ m/s; (b)—$d_0 = 670$ μm, $w_0 = 1.31$ m/s

dimensions of 80-140 μm. At increase of wire feed rate up to 9 m/min (mode #2), the main bulk of particles is of 60-90 μm size. Here, dispersion of particle distribution by velocity and temperature turns out to be smaller, i.e., coating will be formed by a flow of particles of practically the same size, having close values of velocity and tem-

perature. Note that part of particles approaching the substrate has the velocity exceeding that of the main particles bulk by 1.5-2 times and more. Accordingly, such particle sizes turn out to be much smaller than the average particle size in a dispersed flow. As to particle temperature, as was mentioned above at analysis of results shown in Fig. 4, the greater part of them at the moment of collision with the substrate has the temperature, corresponding to material boiling temperature (3133 K), or slightly exceeding it which is typical for particles of smaller-sized fractions.

Proceeding from the calculated data, it is possible to estimate the probability of collision of droplets and their fragments at their motion in a plasma jet. The following expression can be used

$$P_c(T \in (t, t+dt)) = N\pi\bar{d}^2\bar{v}dt, \quad \text{(Eq 32)}$$

determining probability of collision P_c during time dt of particles of an average diameter$\bar{d}$, velocity $\bar{v}$, and volume concentration N. Considering that the calculated average particle diameter is approximately 100 μm, their average motion velocity is 70 m/s, and choosing dt equal to the average in-flight time of particles, the average number of particles in the flow is in the interval of [700 – 1200] (depending on wire feed rate). Consequently, the probability of their collision is in the interval of (7-12) $\times$ 10^{-3}, which justifies the assumption of non-colliding particles and fragments.

4.1 Comparison with Experimental Data

Comparison of calculated size distribution of particles at spraying distance with experimentally measured ones was performed for experimental verification of the proposed mathematical model of heating, movement, and breakup of molten particles. Experimental study of the process of plasma-arc wire spraying was performed using steel wire of 1.6-mm diameter (Sv-08A). Particles were collected by spraying of a wire into water, and particle size distribution was determined by mesh analysis with particle separation into 25-45, 45-75, 75-100, and more than 100 μm fractions with their subsequent weighing. Experimental conditions are summarized in Table 2.

Table 2 Experimental conditions of plasma-arc spraying

No	Current, A	Voltage, V	Flow rate, [Ar], L/min	Wire feed rate, m/min	Wire diameter, mm	Distance to wire, z_0, mm
1	260	60	20	9	1.6	10
2	220	55				10
3	300	62				10
4	220	60				12

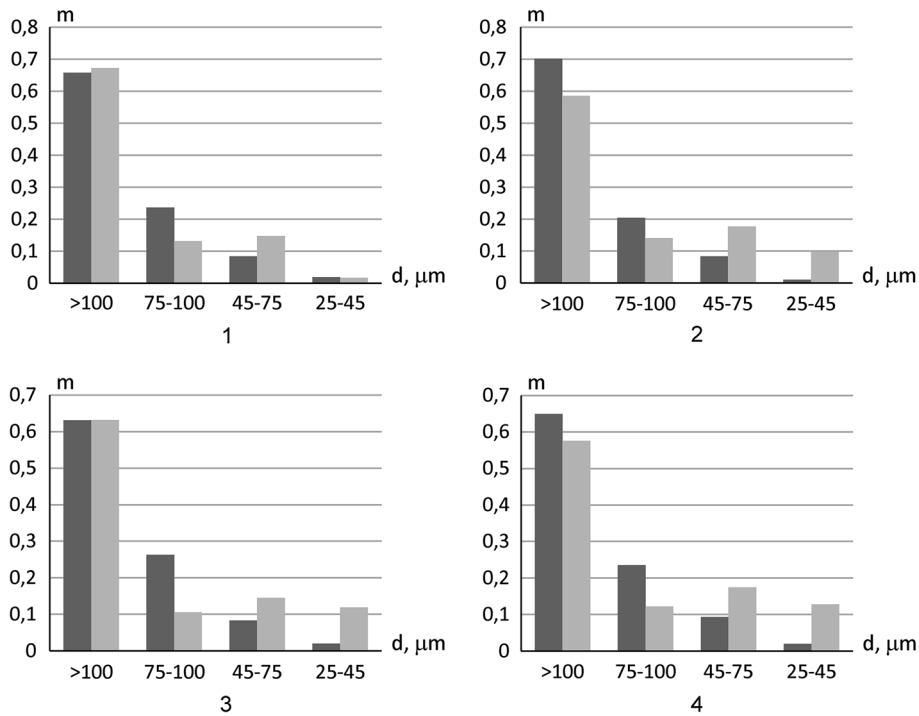

Fig. 7 Comparison of calculated (dark grey bar) and experimental (light grey bar) data by size distribution of products of plasma-arc spraying of wire at spraying distance of 150 mm (histograms 1-4 correspond to spraying modes given in Table 2)

At computer modeling of the process of plasma-arc spraying for mode parameters given in Table 2, characteristics of plasma jet generated by the plasmatron (Ref 30) and parameters of droplets stripped off the wire (Ref 9, 10) were determined, and then their behavior in the plasma jet was modeled. Figure 7 gives experimentally determined and corresponding to them calculated values of particle mass fraction m within the above-mentioned fractions. As follows from comparison of the data given in this Figure, the proposed mathematical model quite well describes behavior of molten particles in the plasma flow, allowing for their breakup. At the same time, certain discrepancy between the calculated and experimental data concerning formation of fragments of very small sizes (<45 μm) should be noted. One can say that analysis of experimental results of spraying into water requires taking into account the not-spherical form of solidified particles due to deformation of droplets when they collide with the water. Furthermore, it suggests the need for further development of the models of liquid particle breaking up in the plasma flow. In particular, it concerns breakup criteria and time characteristics, as well as breakage distribution function.

5. Conclusions

1. The mathematical model was developed, describing the processes of heat and dynamic interaction of plasma jet with molten particles formed at plasma-arc spraying of wire consumables. This model allows determination of velocity, trajectories and heat state of liquid particles, allowing for their aerodynamic breakup in the plasma. Comparison of results of computer modeling of molten metal particle behavior in the plasma jet with experimental data showed that they are in quite good agreement.
2. Allowing for deformation and breakup of molten particles within the proposed model provides an explanation for formation of fragments of dimensions much smaller (by 6 or more times) than those of the droplets, detached from the molten wire tip in plasma-arc spraying that is observed experimentally.
3. Breakup of molten metal droplets detached from the sprayed wire proceeds by the following scenario. In the first region of plasma jet (at $z < 60$ mm), when Weber number for the particles exceeds the critical value, their breakup is practically instantaneous, then (at 60 mm $< z <$ 120 mm) the fragments are exposed to smoothly increasing of aerodynamic drag force due to a change of their shape that, after a certain time, leads to their subsequent breakup, which is over at about 120-mm distance from plasmatron nozzle edge.
4. Numerical analysis of molten particle behavior in plasma-arc wire spraying showed that at plasmatron operation at 200 A current and plasma gas flow rate of 1 m^3/h the optimum wire feeding rate into the plasma arc (in terms of achieving the most uniform dispersed composition of particles forming the coating) is 9 m/min and more, at which the greater part of the particles at spraying distance of 150 mm will have a diameter of 50-100 μm and the velocity of collision with the substrate of 100-180 m/s, at temperature slightly higher than temperature of their material boiling (3133 K).

References

1. L. Pawlowski, *Science and Engineering of Thermal Spray Coatings*, 2nd ed., Wiley, New York, 2008
2. R.I. Nigmatulin, *Dynamics of Multiphase Media*, Vol 1, Taylor & Francis, Philadelphia, 1990
3. Yu.S. Borisov, I.V. Krivtsun, A.F. Muzhichenko, E. Lugscheider, and U. Eritt, Computer Modelling of the Plasma Spraying Process, *Paton Weld. J.*, 2000, **12**, p 40-50
4. K. Remesh, S.C.M. Yu, H.W. Ng, and C.C. Berndt, Computational Study and Experimental Comparison of the In-flight Particle Behavior for an External Injection Plasma Spray Process, *J. Therm. Spray Technol.*, 2003, **12**(4), p 508-522
5. H.-P. Li and X. Chen, Three-dimensional Simulation of a Plasma Jet with Transverse Particle and Carrier Gas Injection, *Thin Solid Films*, 2001, **390**, p 175-180
6. Yu.S. Borisov, A.S. Zatserkovny, and I.V. Krivtsun, Mathematical Modelling of the Process of Plasma Spraying of Composite Powders Allowing for the Exothermic Reaction of Synthesis of Coating Material, *Paton Weld. J.*, 2004, **1**, p 22-24
7. Yu. Borisov, A. Bushma, and I. Krivtsun, Modeling of Motion and Heating of Powder Particles in Laser, Plasma, and Hybrid Spraying, *J. Therm. Spray Technol.*, 2006, **15**(4), p 553-558
8. Yu.S. Korobov, V.N. Boronenkov, Расчет параметров движения, нагрева и окисления частиц при электродуговой металлизации (Calculation of the parameters of movement, heating and oxidation of particles at electric-arc metalizing), *Svarochnoje proizvodstvo*, 1998, No 9, p 9-13. (in Russian)
9. M.Yu. Kharlamov, I.V. Krivtsun, V.N. Korzhik, and S.V. Petrov, Formation of Liquid Metal Film at the Tip of Wire-anode in Plasma-arc Spraying, *Paton Weld. J.*, 2011, **12**, p 2-6
10. M.Yu. Kharlamov, I.V. Krivtsun, and V.N. Korzhyk, Dynamic Model of the Wire Dispersion Process in Plasma-Arc Spraying, *J. Therm. Spray Technol.*, 2014, **23**(3), p 420-430
11. E. Pfender and C.H. Chang, Plasma Spray Jets and Plasma-Particulate Interaction: Modeling and Experiments, *Thermal Spray: Meeting the Challenges of the 21st Century*, C. Coddet, Ed., May 25-29, 1998 (Nice, France), ASM International, Materials Park, 1998, p 315-327
12. L.D. Landau, E.M. Lifshitz, *Fluid Mechanics*, 2nd ed. (Course of Theoretical Physics, Vol. 6), Butterworth-Heinemann, Boston, 1987
13. R. Schmehl, Advanced Modeling of Droplet Deformation and Breakup for CFD Analysis of Mixture Preparation, ILASS-Europe 2002, September 9-11, 2002 (Zürich, Schweiz), ILASS, 2002, p 1-10. http://www.ilasseurope.org/ICLASS/ilass2002/papers/012.pdf)
14. R. Clift, J.R. Grace, M.E. Weber, *Bubbles, Droplets, and Particles*, Dover Publications, New York, 2005
15. B.J. O'Donnel and B.T. Helenbrook, Drag on Ellipsoids at Finite Reynolds Number, *Atomization Sprays*, 2005, **15**(4), p 363-376
16. E.E. Michaelides, *Particles, Bubbles and Droplets: Their Motion, Heat And Mass Transfer*, World Scientific Publ., New Jersey, 2006
17. A.A. Samarskii and B.D. Moiseyenko, An Economic Continuous Calculation Scheme for the Stefan Multidimensional Problem, *USSR Comput Math. Math. Phys.*, 1965, **5**(5), p 43-58
18. S.S. Kutateladze, *Fundamentals of Heat Transfer*, Academic Press, New York, 1963
19. S.V. Dresvin, A.V. Donskoj, V.M. Goldfarb, and V.S. Klubnikin, Физика и техника низкотемпературной плазмы (Physics and

Technology of Low-temperature Plasma), Atomizdat, 1972 (in Russian)
20. Ch.J. Knight, Theoretical Modeling of Rapid Surface Vaporization with Back Pressure, *AIAA J.*, 1979, **17**(5), p 519-523
21. A.M. Podvisotskii, V.V. Dubrovskii, Критические условия разрушения капель газовым потоком (Critical Conditions of Droplet Breakup by Gas Flow), Phys. Aerodispersed Syst, 1998, 37, p 32-37, (in Russian). http://phys.onu.edu.ua/files/journals/fas/articles/37/fas37_podvisockiy.pdf
22. M. Pilch and C.A. Erdman, Use of Breakup Time Data and Velocity History Data to Predict the Maximum Size of Stable Fragments for Acceleration-induced Breakup of Liquid Droplet, *Int. J. Multiphase Flow*, 1987, **13**, p 741-757
23. M.Yu. Kharlamov, I.V. Krivtsun, and V.N. Korzhyk, Numerical Simulation of Movement, Heating and Breakup of Particles, Formed at Wire Dispersion Under the Conditions of Plasma-arc Spraying, *Mathematical Modeling and Information Technologies in Welding and Related Processes: Proceedings of 6th Intern. Conf.*, V.I. Makhnenko, Ed., May 29-June 1, 2012, (Katsiveli, Crimea, Ukraine), E.O. Paton Electric Welding Institute of the NAS of Ukraine, 2012, p 147-155
24. D.R. Guildenbecher, C. López-Rivera, and P.E. Sojka, Secondary Atomization, *Exp. Fluids*, 2009, **46**(3), p 371-402
25. C. Lasheras, C. Eastwood, C. Martinez-Bazán, and J.L. Montañés, A Review of Statistical Models for the Break-up of an Immiscible Fluid Immersed into a Fully Developed Turbulent Flow, *Int. J. Multiphase Flow*, 2002, **28**(2), p 247-278
26. J.M. Marchetti, L.E. Patruno, H.A. Jakobsen, and H.F. Svendsen, Mathematical Framework for Higher Order Breakage Scenarios, *Chem. Eng. Sci.*, 2010, **65**, p 5881-5886
27. R. Andersson and B. Andersson, On the Breakup of Fluid Particles in Turbulent Flows, *AIChE J.*, 2006, **52**(6), p 2020-2030
28. H. Bahmanyar and M.J. Slater, Studies of Droplet Break-up in Liquid-Liquid Systems in a Rotating Disc Contactor. Part I: Condition of no Mass Transfer, *Chem. Eng. Technol.*, 1991, **14**, p 79-89
29. P.J. Hill and K.M. Ng, Statistics of Multiple Particle Breakage, *AIChE J.*, 1996, **42**(6), p 1600-1611
30. M.Yu. Kharlamov, I.V. Krivtsun, V.N. Korzhik, S.V. Petrov, and A.I. Demianov, Mathematical Model of Arc Plasma Generated by Plasmatron with Anode Wire, *Paton Weld. J.*, 2007, **12**, p 9-14
31. J. Hu and H.L. Tsai, Heat and Mass Transfer in Gas Metal Arc Welding. Part I: The Arc, *Int. J Heat Mass Transfer*, 2007, **50**(5–6), p 833-846